

# Probing atomic 'quantum grating' by collisions with charged projectiles

S. F. Zhang<sup>1</sup>, B. Najjari<sup>1</sup>, X. Ma<sup>1</sup> and A. B. Voitkiv<sup>2\*</sup>

<sup>1</sup> *Institute of Modern Physics, Chinese Academy of Sciences, Lanzhou 730000, China*

<sup>2</sup> *Institute for Theoretical Physics I, Heinrich-Heine-University of Düsseldorf,  
Universitätsstrasse 1, 40225 Düsseldorf, Germany*

(Dated: February 8, 2022)

## Abstract

The wave function of an atom passed through a diffraction grating acquires a regular space structure and the interaction of another particle with this atom can be thought of as scattering on a 'quantum grating' composed of a single atom. Probing this 'grating' by collisions with charged projectiles reveals interference effects due to coherent contributions of its 'slits' to the transition amplitude. In particular, the spectra of electrons emitted from the atom in collisions with swift ions exhibit a pronounced interference pattern whose shape can be extremely sensitive to the collision velocity.

PACS numbers: PACS:34.10.+x, 34.50.Fa

## I. INTRODUCTION

One of the fundamental concepts of quantum physics is the wave-particle duality: all atomic objects exhibit both particle and wave properties. It was proposed by Louis de Broglie [1] in 1923. Since then a number of experiments confirmed the wave nature of various atomic particles ranging from electrons [2, 3] to huge molecules consisting of many thousands of atoms [4].

In most of these experiments atomic particles were detected after passing through slits (a diffraction grating). In this phenomenon, which is essentially similar to the famous Young's double-slits interference of light [5], the coherent addition of the amplitudes for different quantum paths leads to interference in the detection probabilities clearly demonstrating the wave-like behaviour of the particles.

The diffraction gratings employed in these experiments were naturally macroscopic. Their microscopic analogs can be found in the atomic world. For instance, a diatomic molecule in processes, where its internal state does not change, may play essentially the same role as the Young's double slits in the interaction with light. Since interference effects in processes involving such molecules arise also when their internal state change, it is obvious that – despite much smaller size – these microscopic 'slits' are associated with richer interference effects. Therefore, beginning with the work of [6]-[7], very significant efforts have been devoted to exploring various interference phenomena arising when particles interact with such molecules (see e.g. [8]-[26]).

A qualitatively different type of microscopic 'grating' can be obtained by letting an atom to pass through a macroscopic diffraction grating. Indeed, the wave function of the atom acquires a periodic space structure. As a result, the interaction of another particle with this

atom can be viewed as scattering of the former on an object which can be called a 'quantum grating'. Like its macroscopic counterpart it possesses a periodic structure, which consists of stronger and weaker interacting parts corresponding to respectively larger and smaller values of the atomic probability density but is constructed just of a single atom. Thus, the structured probability amplitude of a single atom plays now essentially the role of a structured macroscopic piece of matter in usual gratings.

In this communication we explore some properties of an atomic quantum grating by probing it by the Coulomb interaction in collisions with swift charged (structureless) projectiles. Interference effects, caused by coherent contributions to the transition amplitude from different 'slits' of the quantum grating, will be considered for elastic as well as inelastic collisions. It, in particular, will be shown that the spectrum of electrons emitted in ionizing collisions exhibits pronounced ring-like structures whose shape can be extremely sensitive to the value of the collision velocity.

Atomic units are used throughout except where otherwise stated.

## II. GENERAL CONSIDERATION

Let an atom with a momentum  $\mathbf{P}_a^i = (0, P_a^i, 0)$  pass through a macroscopic diffraction grating. The grating is located in the  $(x-z)$ -plane and consists of  $N_0$  slits along the  $z$ -direction (see Fig. 1). The dimensions of the slits are  $a$  and  $b$  (along the  $z$ - and  $x$ -directions, respectively), the period of the grating is  $d$ .

Before the diffraction grating the wavefunction  $\psi(\mathbf{R}_a, \mathbf{r}_e, t)$  of the incident atom is given by

$$\begin{aligned}\psi(\mathbf{R}_a, \mathbf{r}_e, t) &= \psi_{in}(\mathbf{R}_a, \mathbf{r}_e, t) \\ &= A \exp(i(\mathbf{P}_a^i \cdot \mathbf{R}_a - E_a^i t)) \phi_i(\mathbf{r}_e - \mathbf{R}_a) \langle 1 | \end{aligned}$$

where  $A$  is the normalization constant,  $\mathbf{R}_a = (X_a, Y_a, Z_a)$ , where  $X_a = R_a \sin \vartheta_{\mathbf{R}_a} \cos \varphi_{\mathbf{R}_a}$ ,  $Y_a =$

\*Electronic address: voitkiv@tp1.uni-duesseldorf.de

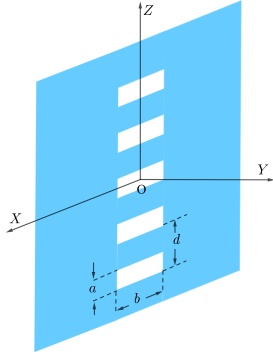


FIG. 1: A diffraction grating with slits located in the  $x$ - $z$  plane,  $a$  and  $b$  are the slit dimensions and  $d$  is the period of the grating.

$R_a \sin \vartheta_{\mathbf{R}_a} \sin \varphi_{\mathbf{R}_a}$  and  $Z_a = R_a \cos \vartheta_{\mathbf{R}_a}$ , is the coordinate of the atomic center-of-mass,  $\mathbf{r}_e$  and  $\mathbf{R}_N$  are the position vectors of the atomic electron and the atomic nucleus, respectively; the origin of the coordinate system is placed in the middle of the diffraction grating (see Fig. 1). Further,  $\phi_i$  is the initial atomic internal state with an energy  $\varepsilon_i$  and  $E_a^i = (\mathbf{P}_a^i)^2/(2M_A) + \varepsilon_i$  is the total initial energy of the atom with  $M_A$  being the atomic mass.

Using the Huygens-Fresnel principle we obtain that after the passage through the grating the wave function of the atom at asymptotically large distances ( $R_a \gg \max\{N_0 d, b\}$ ) can be approximated as

$$\begin{aligned} \psi(\mathbf{R}_a, \mathbf{r}_e, t) &= \psi_{diff}(\mathbf{R}_a, \mathbf{r}_e, t) \\ &= \frac{4A}{R_a} \exp(i(P_a^i R_a - E_a^i t)) \\ &\quad \times \frac{\sin\left(\frac{P_a^i a Z_a}{2 R_a}\right)}{P_a^i \frac{Z_a}{R_a}} \frac{\sin\left(\frac{P_a^i b X_a}{2 R_a}\right)}{P_a^i \frac{X_a}{R_a}} \\ &\quad \times \frac{\sin\left(N_0 \frac{P_a^i d Z_a}{2 R_a}\right)}{\sin\left(\frac{P_a^i d Z_a}{2 R_a}\right)} \phi_i(\mathbf{r}_e - \mathbf{R}_N). \end{aligned} \quad (2)$$

We note that the application of the Huygens-Fresnel principle to describe (optical) diffraction is known to yield excellent results provided the wavelength of light is smaller than  $\min\{a, b\}$ . In what follows we assume that  $P_a^i \simeq 10 - 100$  a.u. and the wavelength of the atom,  $\lambda_a^i = 1/P_a^i$ , will certainly be much smaller than  $\min\{a, b\}$  which enables one to expect that (2) represents a good approximation for the wave function at asymptotically large distances between the atom and the grating ( $R_a \gg \max\{N_0 d, b\}$ ).

As it follows from (2) the wave function of the atom acquired – due to diffraction – a regular space structure. This structure can be unveiled in many ways. In what follows we consider how it can be probed by letting the atom to interact with a projectile which we take here as a point-like charged particle (an electron or a bare nucleus).

Assuming that the energy of the projectile is suffi-

ciently high, we approximate its initial and final states by plane waves

$$\begin{aligned} \Phi_i(\mathbf{R}_p, t) &= \frac{1}{\sqrt{V_p}} \exp(i(\mathbf{p}_p^i \cdot \mathbf{R}_p - \varepsilon_p^i t)) \\ \Phi_f(\mathbf{R}_p, t) &= \frac{1}{\sqrt{V_p}} \exp(i(\mathbf{p}_p^f \cdot \mathbf{R}_p - \varepsilon_p^f t)). \end{aligned} \quad (3)$$

Here  $\mathbf{R}_p$ ,  $\mathbf{p}_p^i$  and  $\varepsilon_p^i = \mathbf{p}_p^{i2}/(2M_p)$  ( $\mathbf{p}_p^f$  and  $\varepsilon_p^f = \mathbf{p}_p^{f2}/(2M_p)$ ) are the position vector, the initial (final) momentum and energy, respectively, of the projectile,  $M_p$  is its mass and  $V_p$  is the normalization volume.

Assuming that the momentum of the atom after the collision is detected, we take its final state as a product of a plane wave, which describes the motion of its center-of-mass, and a final internal state of the atom  $\phi_f$  with an energy  $\varepsilon_f$ ,

$$\psi_f(\mathbf{R}_a, \mathbf{r}_e, t) = \frac{\exp(i(\mathbf{P}_a^f \cdot \mathbf{R}_a - E_a^f t))}{\sqrt{V_a}} \phi_f(\mathbf{r}_e - \mathbf{R}_N), \quad (4)$$

where  $\mathbf{P}_a^f$  and  $E_a^f = (\mathbf{P}_a^f)^2/(2M_A) + \varepsilon_f$  are the final momentum and energy of the atom, respectively, and  $V_a$  is the normalization volume. The state  $\phi_f$  can be either a bound or continuum state; the latter case corresponds to ionization.

In the first order of perturbation theory the transition amplitude reads

$$S_{fi} = -i \int_{-\infty}^{+\infty} dt \langle \Psi_f(t) | \hat{W} | \Psi_i(t) \rangle. \quad (5)$$

Here  $\Psi_i(t) = \psi_{diff}(\mathbf{R}_a, \mathbf{r}_e, t) \Phi_i(\mathbf{R}_p, t)$  and  $\Psi_f(t) = \psi_f(\mathbf{R}_a, \mathbf{r}_e, t) \Phi_f(\mathbf{R}_p, t)$  are the initial and final states, respectively, of the noninteracting "atom + projectile" system and  $\hat{W} = -Z_p/|\mathbf{r}_e - \mathbf{R}_p| + Z_p Z_N/|\mathbf{R}_N - \mathbf{R}_p|$ , where  $Z_p$  ( $Z_N$ ) is the charge of the projectile (the atomic nucleus), is the interaction between them.

Let the target and projectile beams cross at a distance  $D$  from the grating. At this distance a single target atom is localized (along the  $z$ -axis) within a spot whose size  $\Delta_z$  can be estimated from the form of the state (2) and is roughly given by  $\Delta_z \simeq D/(P_a^i a) \sim D \lambda_a^i/a$ . Taking  $D \simeq 200 - 1000$  mm,  $a \simeq 10^{-3} - 0.1$  mm and  $P_a^i \simeq 10 - 100$  a.u. we obtain  $\Delta_z \sim 10^{-7} - 10^{-3}$  mm. This value is much smaller than the size  $L_z = N_0 d (\simeq 10^{-2} - 1$  mm) of the macroscopic grating along the  $z$ -axis. Comparing  $\Delta_z$  and  $L_z$  we see that the typical size of the target spot, which produced by all target atoms passed through the grating, is essentially determined by  $N_0 d \sim 10^{-2} - 1$  mm and thus is much smaller than the distance  $D$ .

A similar consideration shows that for a typical size of the target spot  $\Delta_x$  along the  $x$ -axis one obtains  $\Delta_x \simeq \frac{a}{b} \Delta_z$  and, assuming  $b \simeq a$ , one has  $\Delta_x \sim 10^{-7} - 10^{-3}$  mm.

Using the above estimates and also noting that the diameter of the projectile beam in collisional experiments

is typically of the order of 1 mm (see e.g. [27]) we obtain that each dimension of the interaction volume (the space volume where the beams cross) is much smaller than the distance  $D$  between its center and the macroscopic diffraction grating.

Taking all this into account it is convenient to introduce a new coordinate system with the origin placed in the center of the interaction volume. The new (primed) and old (unprimed) coordinates of the particles are related by  $\mathbf{R}'_a = \mathbf{R}_a - \mathbf{D}$ ,  $\mathbf{R}'_p = \mathbf{R}_p - \mathbf{D}$ ,  $\mathbf{r}'_e = \mathbf{r}_e - \mathbf{D}$ ,  $\mathbf{R}'_N = \mathbf{R}_N - \mathbf{D}$ , where  $\mathbf{D} = (0, D, 0)$ . The state of the diffracted atom now reads

$$\begin{aligned} \psi_{diff}(\mathbf{R}'_a, t) \approx & 4A \frac{\exp(i P_a^i D)}{D} \exp(i(P_a Y' - E_a^i t)) \\ & \times \frac{\sin\left(\frac{P_a^i b X'}{2D}\right)}{P_a^i \frac{X'}{D}} \frac{\sin\left(\frac{P_a^i a Z'}{2D}\right)}{P_a^i \frac{Z'}{D}} \\ & \times \frac{\sin\left(N_0 \frac{P_a^i d Z'}{2D}\right)}{\sin\left(\frac{P_a^i d Z'}{2D}\right)} \phi_i(\mathbf{r}'_e - \mathbf{R}'_N). \end{aligned} \quad (6)$$

The form of the states (3)-(4) in the new coordinates are obvious.

The evaluation of the integrals over the interaction volume and time in (5) results in

$$\begin{aligned} S_{fi} = & 2^6 \pi^3 A i \delta((E_a^f + \varepsilon_p^f) - (E_a^i + \varepsilon_p^i)) \\ & \times \frac{\langle \phi_f(\boldsymbol{\xi}) | \exp(i\mathbf{q} \cdot \boldsymbol{\xi}) | \phi_i(\boldsymbol{\xi}) \rangle}{q^2} F_b(q_x - P_{a,x}^f) \\ & \times \frac{\exp(i P_a^i D)}{D} \times \delta(P_a^i + q_y - P_{a,y}^f) \\ & \times \sum_n F_a(q_z - P_{a,z}^f - P_a^i d n / D), \end{aligned} \quad (7)$$

where  $\boldsymbol{\xi} = \mathbf{r}'_e - \mathbf{R}'_N$ ,  $\mathbf{q} = (q_x, q_y, q_z) = \mathbf{p}_p^i - \mathbf{p}_p^f = (p_{p,x}^i - p_{p,x}^f, p_{p,y}^i - p_{p,y}^f, p_{p,z}^i - p_{p,z}^f)$  is the change in the projectile momentum (= the momentum transfer to the atom) and

$$F_\alpha(\eta) = \begin{cases} \pi; & |\eta| < \frac{P_a^i \alpha}{2D} \\ \pi/2; & |\eta| = \frac{P_a^i \alpha}{2D} \\ 0; & |\eta| > \frac{P_a^i \alpha}{2D}, \end{cases} \quad (8)$$

where  $\alpha = a, b$ . It follows from (7)-(8) that along the  $x$ - and  $z$ -directions there are uncertainties,  $\Delta P_x = P_a^i b / D$  and  $\Delta P_z = P_a^i a / D$ , in the momentum balance in the collision. This is caused by the (uncontrolled) momentum exchange between the atom and the macroscopic diffraction grating resulting in an uncertainty in the momentum of the atom passed through it. However, the energy balance in the collision does not possess an uncertainty because the macroscopic grating, which has essentially infinite (on the atomic scale) mass and is initially at rest, does not participate in the energy exchange.

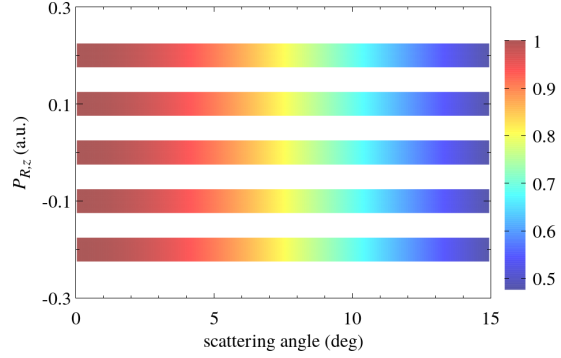


FIG. 2: The differential cross section for elastic scattering of 300 eV electrons incident along the  $x$ -axis on Xe atoms ( $P_a^i = 100$  a.u.) passed through a diffraction grating with  $a = b = d/2 = 0.1$  mm and  $N_0 = 5$ .  $D = 200$  mm. The cross section is given in relative units with its intensity ranging from 0 to 1.

### III. RESULTS AND DISCUSSION

#### A. Elastic collisions with electrons

Fig. 2 displays the elastic cross section, differential in the projectile scattering angle and the component  $P_{a,z}^f$  of the final atomic momentum, for 300 eV electrons incident along the  $x$ -axis on Xe atoms which passed through a diffraction grating. A clear interference pattern observed in the cross section is caused by the coherent addition of the contributions of the different 'slits' of the atomic quantum grating to the process of electron scattering.

#### B. Ionization in collisions with bare ions

We now consider collisions of atoms with bare ions resulting in atomic ionization. Using the transition amplitude (7) we obtain the fully differential cross section for atomic ionization

$$\begin{aligned} \frac{d\sigma}{d^3\mathbf{q} d^3\mathbf{P}_R d^3\mathbf{k}} = & 2^{12} \pi^4 A^2 \frac{Z_p^2}{v P_a^i{}^2} \\ & \times \frac{|\langle \phi_{\mathbf{k}}(\boldsymbol{\xi}) | \exp(i\mathbf{q} \cdot \boldsymbol{\xi}) | \phi_i(\boldsymbol{\xi}) \rangle|^2}{q^4} \\ & \times \delta(P_a^i + q_y - P_{R,y} - k_y) \\ & \times \delta(E_a^f + \varepsilon_p^f - E_a^i - \varepsilon_p^i) \\ & \times F_b^2(q_x - P_{R,x} - k_x) \\ & \times \sum_n F_a^2(B_n). \end{aligned} \quad (9)$$

Here,  $\mathbf{P}_R = (P_{R,x}, P_{R,y}, P_{R,z})$  is the momentum of the target recoil ion,  $\mathbf{k} = (k_x, k_y, k_z)$  is the momentum of the emitted electron, and  $B_n = q_z - P_{R,z} - k_z - P_a^i d n / D$ .

Since  $M_A \gg m_e$  ( $m_e$  is the electron mass) one has  $E_a^f - E_a^i \approx k^2/2 - \varepsilon_i$ . Besides, for collisions with  $|\mathbf{q}| \ll |\mathbf{p}_i|$ , one obtains  $\varepsilon_p^i - \varepsilon_p^f = (\mathbf{p}_i^2 - \mathbf{p}_f^2)/(2M_p) = (\mathbf{p}_i -$

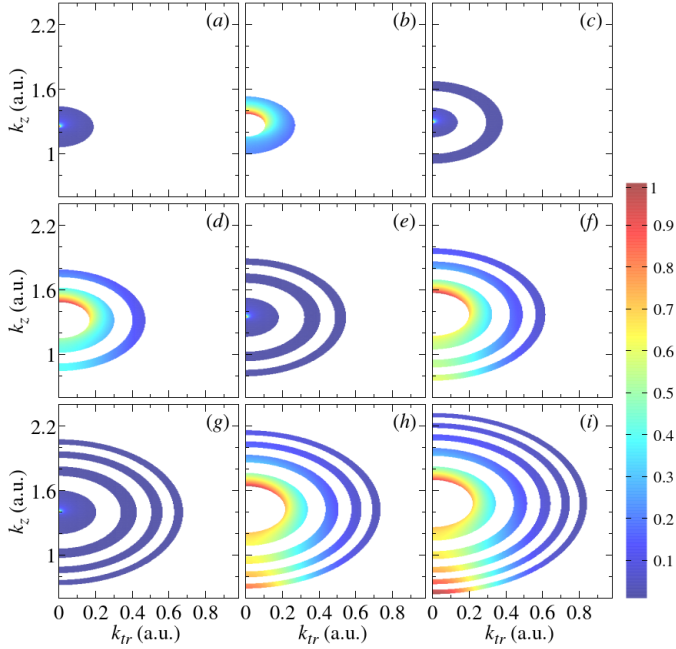


FIG. 3: Spectra of electrons emitted from He atoms ( $P_a^i = 50$  a.u.,  $\varepsilon_i = -0.9$  a.u.) passed through a diffraction grating ( $a = b = d/2 = 0.1$  mm,  $N_0 = 5$ ) in collisions with protons.  $D = 200$  mm,  $P_{R,z} = q_x = q_y = 0$ . The collision velocity  $v = f v_0$ , where  $v_0 = \sqrt{2|\varepsilon_i|}$  and  $f = 0.93$  (a),  $0.94$  (b),  $0.96$  (c),  $0.98$  (d),  $1$  (e),  $1.02$  (f),  $1.04$  (g),  $1.06$  (h),  $1.1$  (i). The spectra are given in relative units with their intensities ranging from 0 to 1.

$\mathbf{p}_f)(\mathbf{p}_i + \mathbf{p}_f)/(2M_p) \approx \mathbf{q} \cdot \mathbf{v}$ . Therefore, the energy delta-function in (9) can be rewritten as  $\frac{1}{v} \delta(q_{\parallel} - (k^2/2 - \varepsilon_i)/v)$ , where  $q_{\parallel} = \mathbf{q} \cdot \mathbf{v}/v$ .

Let the projectile be incident along the  $z$ -direction. Integrating the cross section (9) over  $P_{R,x}$ ,  $P_{R,y}$  and  $q_z$  we obtain

$$\frac{d\sigma}{d^2\mathbf{q}_{\perp} dP_{R,z} d^3\mathbf{k}} \sim \frac{Z_p^2}{v^2} \frac{|\langle \phi_{\mathbf{k}}(\boldsymbol{\xi}) | \exp(i\mathbf{q}_0 \cdot \boldsymbol{\xi}) | \phi_i(\boldsymbol{\xi}) \rangle|^2}{q_0^4} \times \sum_n F_a^2(B_n), \quad (10)$$

where  $\mathbf{q}_0 = (q_x, q_y, q_{min}) = (\mathbf{q}_{\perp}, q_{min})$  with  $q_{min} = (k^2/2 - \varepsilon_i)/v$  and  $B_n = q_{min} - P_{R,z} - k_z - P_a^i n/D$ .

The binary-encounter emission and electron capture to the projectile continuum belong to the most prominent features of ionization (see e.g. [28] and references therein). The former is a two-body ionization mechanism in which the momentum exchange in the collision occurs between the projectile and the electron while the target nucleus/core is merely a spectator:  $P_{R,x} \approx 0$ ,  $P_{R,z} \approx 0$ ,  $P_{R,y} \approx P_a^i$ . In the latter the emitted electron moves with a velocity  $\mathbf{v}_e \approx \mathbf{v}$ , i.e. together with the projectile but without forming a bound state with it.

By analysing the collision momentum balance  $q_{min} \approx P_{R,z} + k_z$  one can convince oneself that, provided  $|\varepsilon_i| = v^2/2$ , these two features are present simultaneously. Such

an interesting situation is considered in Fig. 3 where the cross section  $d\sigma/(d^2\mathbf{q}_{\perp} dP_{R,z} dk_z dk_{\perp})$ , taken at  $P_{R,z} = q_x = q_y = 0$ , is shown as a function of  $k_z$  and  $k_{\perp} = \sqrt{k_x^2 + k_y^2}$  for single ionization of atomic helium by proton projectiles.

As is well known [28], for electron capture to the projectile continuum the interaction between the projectile and the emitted electron is crucial. Since the first order approximation neglects this interaction, the cross section was calculated using the Continuum-Distorted-Wave-Eikonal-Initial-State approach [29] which accounts for this interaction yielding a satisfactory description of this process.

The electron spectrum shown in Fig. 3 exhibits a pronounced interference structure consisting of concentric rings. The center, the width and the number of the rings are determined by the inequalities  $B^- \leq (k_z - v)^2 + k_{\perp}^2 \leq B^+$ , where  $B^{\pm} = v^2 - 2|\varepsilon_i| + 2v P_a^i \frac{d}{D} n \pm v P_a^i \frac{a}{D}$ . This structure arises due to the coherent contributions to the emission from different parts of the atomic quantum grating which strongly interfere in the cross section. The number of the rings, their size and even the relative intensity on them turn out to be extremely sensitive to the magnitude of the collision velocity.

#### IV. CONCLUSIONS

Due to a regular space structure acquired by the wave function of an atom, which passed through a macroscopic diffraction grating, this atom can itself be regarded as a diffraction grating. Compared to macroscopic gratings and even to microscopic gratings represented by molecules, this type is qualitatively different since it consists of just a single atom; the role of the structured "real matter" in the former ones is now mimicked by the structured probability amplitude.

We have considered interference effects appearing when such an atomic quantum grating is probed by collisions with point-like charged projectiles. These effects arise due to the coherent addition of the contributions of different 'slits' of the atomic grating to the transition amplitude and very clearly manifest themselves both in elastic and ionizing collisions.

In particular, interesting patterns arise in the spectra of electrons ejected in collisions with ions in the kinematic range where there is a 'confluence' of the binary-encounter emission and electron capture to the projectile continuum. In such a case a pronounced interference structure appears in the emission spectrum whose shape is extremely sensitive to the magnitude of the collision velocity. This point might potentially be exploited for a very precise determination of this velocity.

As preliminary estimates show, atomic quantum gratings can profoundly manifest themselves also in other basic atomic collision processes (e.g. electron capture to a bound state and projectile-electron loss) as well as in

photoabsorption and photon scattering.

An experimental verification of the theoretical predictions requires both (i) high quality (monochromatic) beams of projectiles and target atoms and (ii) an accurate determination of the momenta of the particles in the final state. While there is no big problem with fulfilling the condition (i) (for instance, the typical energy spread of 10 – 100 keV/u ions can be optimized to a few eV meeting the monochromatic beam criteria), the determination of the final momenta with the necessary accuracy is quite challenging.

In experiments with reaction microscopes helium targets have momenta substantially less than the value  $P_i = 50$  a.u. used here (see Figs. 2 and 3). Smaller  $P_i$  reduce the size and thickness of the rings in Fig. 3 setting even a stronger requirement on the accuracy in the momentum determination. To prepare the initial target moment of  $P_i \sim 50 - 100$  a.u., one could use heavier targets (e.g. Ar or Xe). But for heavy targets the accuracy of the momenta determination is usually of the order of a few atomic units for a reaction microscope equipped with the room-temperature super-sonic gas jet, which is far away from the value of  $\lesssim 0.1$  a.u. necessary to resolve the structures in Figs. 2 and 3. To reach a much

better accuracy a reaction microscope with a precooling super-sonic gas jet can be envisaged.

However, the requirements on the accuracy in the determination of the final momenta can be greatly softened if, instead of target atoms, structured projectiles (e.g.  $\text{He}^+$ ) pass through a macroscopic grating. Due to much higher incident momenta, the uncertainty in the projectile momentum after the diffraction grating will be much larger. For instance, for 25 - 100 KeV/u  $\text{He}^+$  ions passed through a grating with  $a \simeq b \simeq 0.1$  mm, one obtains  $\Delta p_p \simeq p_p^i a/D \simeq 3.5 - 7$  a.u. at  $D = 200$  mm.

## V. ACKNOWLEDGEMENT

We acknowledge the support from the National Key Research and Development Program of China (Grant No. 2017YFA0402300), the CAS President's International Fellowship Initiative and the German Research Foundation (DFG) under Grant No 349581371 (the project VO 1278/4-1). A. B. V. is grateful for the hospitality of the Institute of Modern Physics.

- 
- [1] L. de Broglie, PhD thesis, reprinted in Ann. Found. Louis de Broglie 17, 22 (1992).
  - [2] C. J. Davisson and L. H. Germer, Phys. Rev. 30, 705 (1927).
  - [3] G. P. Thomson, Proceedings of the Royal Society (London) A117, 600 (1928).
  - [4] Y. Y. Fein, F. Geyer, P. Zwick, F. Kialka, S. Pedalino, M. Mayor, S. Gerlich and M. Arndt, Nature Physics, <https://www.nature.com/articles/s41567-019-0663-9> (2019).
  - [5] T. Young, Philosophical Transactions, Nov. 24th 1803.
  - [6] T. F. Tuan and E. Gerjuoy, Phys. Rev. **117**, 756 (1960).
  - [7] H. Cohen and U. Fano, Phys. Rev. 150, 30 (1966).
  - [8] F. Lindner et al, Phys. Rev. Lett. **95** 040401 (2005).
  - [9] K. Kreidi et al, Science **318** 949 (2007).
  - [10] J. Fernandez et al, Phys. Rev. Lett. **98** 043005 (2007).
  - [11] D. Akoury et al., Science 318, 949 (2007).
  - [12] B. Zimmermann et al., Nature Physics 4, 649 (2008).
  - [13] K. Kreidi et al, Phys. Rev. Lett. **100** 133005 (2008).
  - [14] C. D. Lin et al, J. Phys. **B 43**, 122001 (2010).
  - [15] N. A. Cherepkov et al, Phys. Rev. **A 82**, 023420 (2010).
  - [16] D. S. Milne-Brownlie et al, Phys. Rev. Lett. **96** 233201 (2006).
  - [17] N. Stolterfoht et al., Phys. Rev. Lett. 87, 023201 (2001).
  - [18] D. Misra et al., Phys. Rev. Lett. 92, 153201 (2004).
  - [19] C. Dimopoulou et al, Phys. Rev. Lett. **93** 123203 (2004).
  - [20] H. T. Schmidt et al, Phys. Rev. Lett. **101** 083201 (2008).
  - [21] L. Ph. H. Schmidt et al, Phys. Rev. Lett. **101** 173202 (2008).
  - [22] J.S. Alexander et al, Phys. Rev. **A 78** 060701(R) (2008).
  - [23] D. Misra et al, Phys. Rev. Lett. **102** 153201 (2009).
  - [24] A. B. Voitkiv et al, Phys. Rev. Lett. 106, 233202 (2011).
  - [25] S. F. Zhang et al, Phys. Rev. Lett. **112**, 023201 (2014).
  - [26] Y. Gao, S. F. Zhang, X. L. Zhu, et al, Phys. Rev. **A 97**, 020701(R) (2018).
  - [27] D. Fischer, A. B. Voitkiv, R. Moshhammer, and J. Ullrich, Phys. Rev. **A 68**, 032709 (2003).
  - [28] J. H. Macek and S. T. Manson, Chapter 53 in *Springer Handbook on Atomic, Molecular and Optical Physics*. (Springer, Berlin, 2006).
  - [29] D. S. F. Crothers and J. McCann, J. Phys. **B 16** 3229 (1983).